Biochar Derived from *Sesbania sesban* Plant as a Potential Low-Cost Adsorbent for Removal of Methylene Blue

Nguyen Trung Hiep[1], Ta Thi Hoai Thu[2], Lam Thi Thanh Quyen[2], Phan Dinh Dong[1], Tran Tuyet Suong[1], and Thai Phuong Vu[1*]

[1]Research Institute for Sustainable Development, Ho Chi Minh University of Natural Resources and Environment, 236B Le Van Sy, Tan Binh District, Ho Chi Minh City 700000, Vietnam
[2]Faculty of Environment, Ho Chi Minh University of Natural Resources and Environment, 236B Le Van Sy, Tan Binh District, Ho Chi Minh City 700000, Vietnam

ARTICLE INFO

Received: 29 May 2022
Received in revised: 13 Jul 2022
Accepted: 1 Aug 2022
Published online: 14 Sep 2022
DOI: 10.32526/ennrj/20/202200119

Keywords:
Biochar/ Low-cost adsorbent/ Methylene blue/ *Sesbania sesban*

*** Corresponding author:**
E-mail: tpvu@hcmunre.edu.vn

ABSTRACT

In this study, biochar made from the *Sesbania sesban* plant, under slow pyrolysis at 300°C was used to adsorb methylene blue (MB) in aqueous solution. The biochar properties were clarified by diverse analytical methods such as FTIR, SEM, and BET. The results indicated that the surface of biochar was relatively smooth, had porous texture, and stacked evenly. In addition, the biochar had a large specific surface area of 561.8 m^2/g and the pH_{pzc} value was 6.9. The effect of adsorbent dosage, initial pH, contact time, and concentration of dye solution on biochar were investigated. The optimum conditions for MB adsorption were found at the MB concentration of 50 mg/L, initial pH of 11, biochar mass of 0.6 mg, and contact time of 30 min. Under these optimal conditions, MB dye removal efficiency was above 90%. Adsorption isotherm data were fitted with the Langmuir isotherm model (R^2=0.897) suggesting the adsorption was monolayer, and its maximum adsorption capacity was about 6.6 mg/g. The adsorption kinetic models showed that the linear pseudo-second-order by R^2=0.999 was well fitted. The results indicated the enormous potential of *Sesbania sesban* plant to produce biochar as a low-cost and rather high-effective adsorbent for dye removal from wastewater as well as water quality improvement.

1. INTRODUCTION

Presently, removing color from industrial wastewater, particularly from textile and color manufacturers, is an important pollution control measure. Dye wastewater dumped into natural receiving waters may render them unfit for human consumption due to the toxicological challenges caused by harmful dyes to the environment and human health. Methylene blue (MB), for example, is a synthetic dye that is widely employed in medical staining agents, diagnostic examination, and fiber coloring agents in the textile industry (Ahmad et al., 2020). A high dose of MB dye produces major skin problems, eye discomfort, vomiting, decreases cardiac output, renal blood flow, and other side effects (Rahman-Setayesh et al., 2019). Furthermore, MB has poor biodegradability, so it needs to be treated before being discharged into the environment.

The standard water treatment solutions cannot effectively decolorize dyes because of their complex chemical structure and resistance to oxidizing chemicals and light. Hence, these dyes are processed using a variety of procedures commonly employed in industrial effluent treatment, such as membrane process (Liu et al., 2020; Rashidi et al., 2015), solidification (Khayat and Zali-Boeini, 2019), ion exchange (Joseph et al., 2020), electrochemical oxidation (Rodríguez-Narváez et al., 2021), and absorption (Nouri et al., 2021; Saleh et al., 2021). However, among present treatment methods, adsorption is the most effective solution for removing contaminants from an aquatic environment due to its ease of usage and high efficiency (Nodehi et al., 2022; Sarbisheh et al., 2017; Tran et al., 2020). Absorption techniques can especially deal with different types of color. There are many adsorbents have been studied such as activated carbon (Hameed et al., 2007), graphene oxide (Zhang et al., 2011), carbon

Citation: Hiep NT, Thu TTH, Quyen LTT, Dong PD, Suong TT, Vu TP. Biochar derived from *Sesbania sesban* plant as a potential low-cost adsorbent for removal of methylene blue. Environ. Nat. Resour. J. 2022;20(6):611-620. (https://doi.org/10.32526/ennrj/20/202200119)

nanotubes (Li et al., 2013), bentonite (Oussalah and Boukerroui, 2020), and diatomite (Du and Danh, 2021). Furthermore, a numerical study on using low-cost and regeneration adsorbents have been investigated (Abdul et al., 2021; Alorabi et al., 2021; Hussain et al., 2022; Misran et al., 2022).

In recent years, biochar has been evaluated as a highly effective, environmentally safe and cost-effective adsorbent, which is used for water purification and removal of various contamination (Nguyen et al., 2021; Sutar et al., 2022). Biochar is produced by pyrolysis of organic raw materials under conditions in the absence or limitation of oxygen (Meyer et al., 2011). As reported by Lee et al. (2020), the biochar adsorption process is heavily influenced by biomass type, pyrolysis conditions, porosity, and surface functionalities. Moreover, the biochar has distinct qualities such as a huge surface area, a highly porous structure, enhanced surface functional groups, and mineral components. In order to produce biochar, various other biomass has been investigated such as agricultural organic waste, botanical biomass, and animal waste (Ahmad et al., 2020; Liu et al., 2012; Lonappan et al., 2016). However, to our knowledge, the preparation of biochar from *Sesbania sesban* plant has not been studied yet. Therefore, biochar generated from *S. sesban* plant is considered as a new type of biomass with properties that need to be explored. *S. sesban* plant is a scrub that fixes atmospheric N_2 and has both commercial and biological importance (Farghaly et al., 2022; Kwesiga et al., 1999). In Vietnam, the leaves of *S. sesban* are used as feed to augment rice straw in animal diets and as much in home gardens (Dan et al., 2011). *S. sesban* thrives rapidly in wetland areas in the Mekong Delta. Notably, the stem of *S. sesban* has a porous structure, light, and water absorption capacity. It is these unique properties that make *S. sesban* a potential biomass to produce biochar.

This study was carried out to figure out the adsorption potential of biochar derived from *S. sesban* biomass based on the experiments on methylene blue (MB) adsorption. The MB dye was thought as a model for visible pollution due to its strong adsorption onto the materials. The absorption process was carried out at different batch adsorption conditions (adsorbent dosage, initial MB concentration, contact time, and pH) and calculated through adsorption isotherms and kinetics. The biochar was characterized by Fourier transform infrared spectroscopy (FT-IR), scanning electron microscope (SEM) images, and Brunauer-Emmett-Teller (BET) analysis. This research advances our understanding of a new material and suggests a possible adsorbent for the treatment of dye-rich wastewater.

2. METHODOLOGY

2.1 Preparation of biochar and adsorbate

The *S. sesban* plant was harvested from the Mekong delta region in southwestern Vietnam and used to make biochar. *S. sesban* stalks were stripped of their shells and leaves, cut into small pieces, and dried outside for 2-4 days before being cleaned to remove contaminants. Next, the material was dried at 105°C in 24 h. To make biochar from *S. sesban*, the materials were placed in inox cups with lids and heated under oxygen-limited conditions in a muffle furnace (Nabertherm GmbH, model B410, Germany). This muffle furnace was set to heat to 300°C at a rate of 10°C/min, and it was kept there for 2 h. Lastly, the biochar was crushed into small particles and then screened through sieves with a mesh size of 0.15 mm. The biochar derived from *S. sesban* plant was abbreviated as BSS. It was kept in an airtight container until used in adsorption experiments.

Methylene Blue (MB), a cationic dye with a chemical formula of $C_{16}H_{18}ClN_3S$, was chosen as the adsorbate in this research. It was purchased from Xilong Chemical Co., Ltd., China. The MB stock solution (1,000 mg/L) was made with distilled water. The working solutions were made by diluting this stock solution with distilled water to the required concentration.

2.2 Analysis of the biochar characterization

The pH value at the point of zero charge (pH_{pzc}) of the biochar was determined using the solid addition method. Accordingly, around 50 mL of 0.1 M NaCl was prepared in a series of 100 mL Erlenmeyer flasks. The initial pH values (pH_i) were roughly adjusted in the pH range of 2-12 by adding 0.1 M HCl or 0.1 M NaOH solution. Then, 1 g of biochar was added to each 50 mL conical flask. After 24 h of shaking using a rotary shaker at room temperature, the final pH values (pH_f) of the solution were determined. Finally, the difference between pH_i and pH_f ($\Delta pH = pH_i - pH_f$) was plotted against pH_i. The point of zero charge (pH_{pzc}) was defined as the intersection of the plot and the X-axis.

The microscopic surface texture of biochar was examined using a Scanning Electron Microscope (Thermo Scientific, model Prisma E SEM, USA). The functional groups present in the material were

characterized by Fourier Transform Infra-Red spectrometer (Thermo Scientific, model Nicolet iS5, USA). In addition, the specific surface areas of the adsorbent were measured by the Brunauer-Emmett-Teller (BET) method using nitrogen gas adsorption at -196°C as an analyzer.

2.3 Adsorption experiments

Batch experiments were conducted to investigate the efficiency of MB removal in an aqueous solution. The influence of varied reaction conditions on MB removal efficiency were examined by altering the pH solution (viz., 4, 5, 6, 7, 8, 9, 10, 11), contact time (viz., 0, 10, 20, 30, 40, 50, 60 min), biochar dosage (viz., 0.2, 0.4, 0.6, 0.8, 1.0, 1.2 g), and initial MB solution concentration (viz., 20, 30, 40, 50, 60, 70, 80 mg/L). Adsorption studies were carried out in Erlenmeyer flasks containing 50 mL of MB solution in a rotary shaker (Jeio Tech, model OS-2000, Korea) at 150 rpm and 30±2°C. After adsorption, the filter paper was used to get the adsorbent from the suspension. The concentration of filtrate was analyzed by measuring the MB absorbance using a UV-Vis spectrophotometer (Thermo Scientific, model Evolution 350, USA) at a wavelength of maximum absorbance (665 nm). All of the experiments were carried out in triplicates.

The amount of adsorbate at equilibrium, at a particular time and MB removal efficiency, were calculated using the equations (1-3), respectively (Tehubijuluw et al., 2021).

$$\text{The adsorption capacity at equilibrium: } q_e = \frac{C_0 - C_e}{m} \times V \quad (1)$$

$$\text{The adsorption capacity at a particular time: } q_t = \frac{C_0 - C_t}{m} \times V \quad (2)$$

$$\text{Removal efficiency: } H\% = \frac{C_0 - C_e}{C_0} \times 100 \quad (3)$$

Where; q_e is the adsorption capacity at equilibrium, q_t is the adsorption capacity at a particular time, C_0 is the initial MB solution concentration (mg/L), C_e is the equilibrium MB solution concentration (mg/L), C_t is the MB solution concentration (mg/L) at time t, V is the volume of solution (L), and m is the mass of the biochar (g).

2.4 Adsorption isotherm and kinetic models

The Langmuir and Freundlich (Assimeddine et al., 2022; Shayesteh et al., 2016) adsorption isotherm models were used to study the adsorption performance at equilibrium. The non-linear forms of the isotherm models are shown in Equations (4-5).

$$\text{Langmuir adsorption isotherm model: } q_e = \frac{Q_{max} K_L C_e}{1 + K_L C_e} \quad (4)$$

$$\text{Freundlich adsorption isotherm model: } q_e = K_F C_e^{(1/n)} \quad (5)$$

Where; C_e (mg/L) is the equilibrium concentration of the MB, q_e (mg/g) is the amount of MB adsorbed per unit mass of biochar, Q_{max} is maximum adsorption capacity (mg/g), K_L (L/mg) is the Langmuir constant related to the heat of adsorption, K_F [(mg/g)/(mg/L)$^{1/n}$] is the Freundlich adsorption capacity, and 1/n (dimensionless) is a Freundlich intensity parameter.

In terms of adsorption kinetics, pseudo-first-order kinetic model and pseudo-second-order kinetic model were applied to investigate MB adsorption capability onto each adsorbent surface (Shayesteh et al., 2016). The formulas of the models are expressed in non-linear form as follows:

$$\text{Pseudo-first-order kinetic model: } q_t = q_e\left(1 - \exp^{-k_1 t}\right) \quad (6)$$

$$\text{Pseudo-second-order kinetic model: } q_t = \frac{q_e^2 k_2 t}{1 + q_e k_2 t} \quad (7)$$

Where; q_e (mg/g) is the adsorbed amount at equilibrium, q_t (mg/g) the adsorbed amount at time t (min). In addition, k_1 (1/min) and k_2 (g/mg.min) were respectively the rate constants of the two kinetic models.

3. RESULTS AND DISCUSSION

3.1 Characterization of adsorbent

3.1.1 Fourier transforms infrared analysis (FTIR)

The presence of organic functional groups on the surface of BSS were characterized using FTIR analysis. Figure 1 shows the FTIR spectrum of BSS. The broad absorption band at 3,500-3,300 cm^{-1} was expressed with a peak band of about 3,451 cm^{-1} due to O-H vibrations of alcohols, phenols, and carboxylic acids, as in cellulose and lignin. As a result, phenolic and acidic groups were responsible for the adsorption of MB dye on BSS. The small peaks at 2,937 and 2,869 cm^{-1} can be attributed to the C-H stretching (Bhattacharya et al., 2021). The absorption band near 1,640 cm^{-1} corresponds to the C=C stretching vibration from conjugated alkene groups. The peak at 1,450 cm^{-1} may be regarded as a C-H bending vibration caused by the

methyl group. Another band was found at about 1,222 cm^{-1}, which was associated with C-O stretching.

3.1.2 Scanning electron microscopy (SEM)

The morphology of the BSS is presented in the SEM image (Figure 2). The surface of BSS is relatively smooth, porous texture, and stacks evenly. This unique morphological result led to a high surface area. In addition, the block pore structure facilitated MB adsorption.

3.1.3 Specific surface area

The physical properties of BSS were analyzed in order to confirm the specific surface area, pore diameter, and total pore volume (Table 1). The BET results have shown a huge surface area of up to 561.8 m^2/g. This surface area is higher than that of other non-modified biochar. Therefore, it is envisaged that they will have a high adsorption capability to the MB dye in an aqueous solution.

3.1.4 pH zero charge point (pH_{pzc})

The pH_{pzc} (zero charge point pH) describes the pH value at which the surface charge of the adsorbent is zero. This is a vital parameter in adsorption processes that demonstrates the comprehensive effects of functional groups on the surface of biochar. Essentially, when the pH_{pzc} is greater than the solution pH, the adsorbent surface becomes positively charged; conversely, when the pH_{pzc} is less than the solution pH, the adsorbent surface becomes negatively charged. The result of this research showed that the pH_{pzc} value of the BSS was roughly 6.9 (Figure 3). When the solution pH was above 6.9, the surface of the adsorbent was negatively charged. As a result, the BSS efficiently adsorb a cationic MB dye.

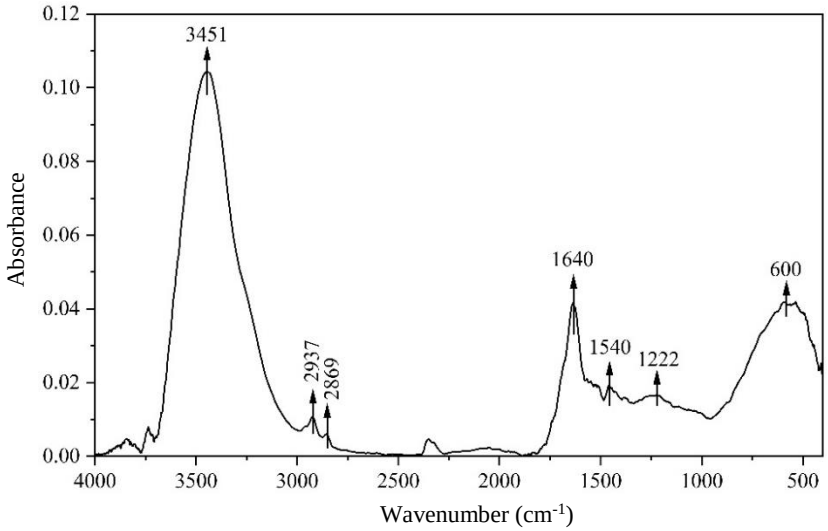

Figure 1. FTIR spectra of biochar

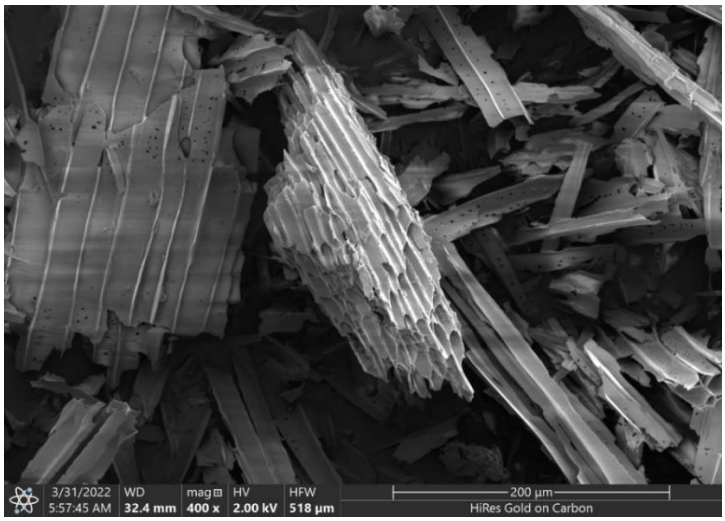

Figure 2. The SEM morphology of BSS

Table 1. The physical properties of BSS for N_2 adsorption

Parameters	Value
BET specific surface area (m^2/g)	561.8
Total pore volume (cm^3/g)	0.5
Pore diameter (nm)	3.7

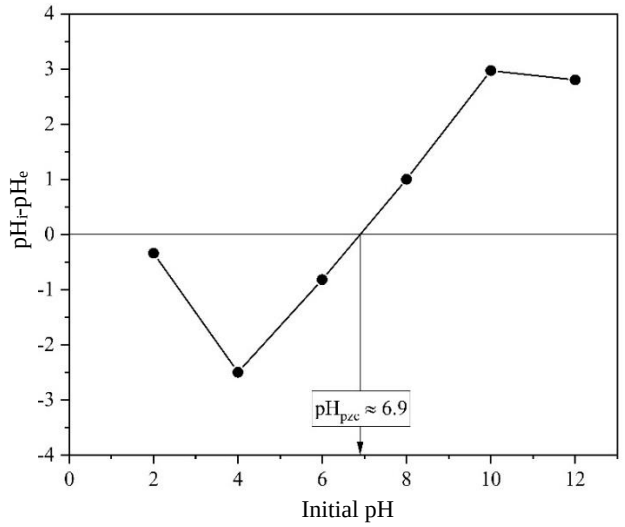

Figure 3. The pH zero charge point (pH_{pzc}) of BSS

3.2 Adsorption performance

3.2.1 Influence of pH on adsorption

The initial solution pH is a vital parameter in the adsorption process which can affect the surface charge of the biochar as well as the chemistry of the adsorbate. Furthermore, the influence of pH on MB adsorption might reveal information on adsorption mechanisms. Figure 4(a) shows the experimental performance of MB adsorption at different pH conditions. The results present an increasing trend in the MB removal efficiency and adsorption capacity of biochar as the pH increased from 4 to 11. This trend was consistent with the results of previous studies (Assimeddine et al., 2022; Dawood et al., 2016; Huang et al., 2018). The removal efficiency of MB was low ~66% at acidic pH (range 4-5). As the pH of the MB solution approached 11, the removal efficiency was approximately 90% and the adsorption capacity reached 3.4 mg/g. These results can be explained when the solution pH is above 6.9 ($pH_{solution} > pH_{pzc}$), the biochar surface is negatively charged, which promotes adsorption of the MB dye. This adsorption is principally caused by electrostatic attraction between the surface adsorbent and the positive charge MB molecules.

3.2.2 Influence of contact time on adsorption

The MB dye adsorption of biochar was investigated in the contact time of 10-60 min, pH of 11, and the adsorbent dosage of 0.4 g was mixed with the initial MB concentration of 30 mg/L. As indicated in Figure 4(b), the MB dye removal efficiency and adsorption capacity of biochar increased rapidly in the first 10 min, and then progressively stabilized. The first quick adsorption is caused by a physical mechanism involving solid-to-liquid mass transfer. The ensuing stabilization phase shows deterioration in physical adsorption with equilibrium and minor desorption of MB dye. In this study, the acceptable contact time for adsorption to reach an equilibrium state was 30 min. At this time, MB adsorption efficiency and adsorption capacity of biochar reached approximately 94% and 3.5 mg/g, respectively.

3.2.3 Influence of biochar dosage on adsorption

The MB dye adsorption performance at the different dosages of biochar is shown in Figure 4(c). The removal efficiency of MB dye increased rapidly (from 62.7±2.7% to 92.1±0.4%) when the biochar dosage was in the range of 0.2-0.4 g (per 50 mL of MB solution). The rise in adsorption efficiency with increasing adsorbent dosage was explained by the enhancement in the higher number of adsorption sites. When biochar dosage was increased from 0.4 to 0.8 g, the performance gradually stabled. However, when the biochar mass was increased to 1.2 g, the treatment efficiency tended to decrease slightly. The MB dye adsorption was enhanced insignificantly when the biochar dose was raised to a specified amount because the adsorbent layers overlapped and concealed the adsorbent active sites. The tendency to simultaneously increase the adsorption capacity and MB removal efficiency when increasing the amount of adsorbent was also found in some previous studies (Inyang et al., 2014; Lonappan et al., 2016; Sun et al., 2013). In this study, to save adsorbent cost, biochar in the amount of 0.6 g was suggested to be used for further experiments. At an adsorbent dosage of 0.6 g (per 50 mL of MB solution), MB dye adsorption efficiency and adsorption capacity of biochar reached approximately 95% and 3.6 mg/g, respectively.

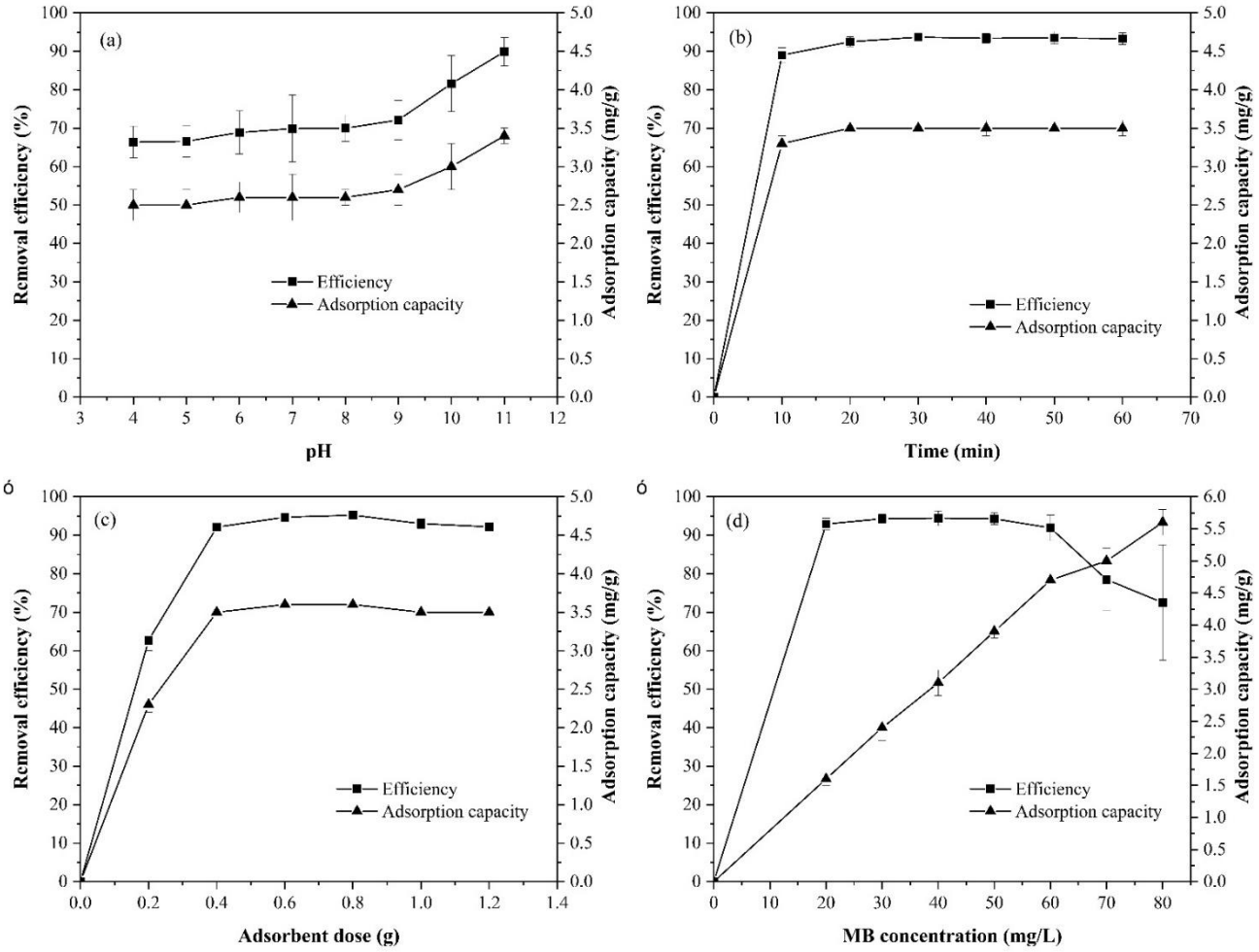

Figure 4. The influence of different experimental conditions on MB adsorption by biochar: (a) Initial pH solution, (b) Contact time, (c) Biochar dosage, and (d) MB concentration

3.2.4 Influence of initial MB concentration on adsorption

The effect of initial concentrations is an important factor for MB dye adsorption. In this study, MB concentrations were investigated in the range of 20-80 mg/L. As observed in Figure 4(c), the MB removal efficiency was over 90% when the initial dye concentration rose from 20 to 60 mg/L. Simultaneously, the adsorption capacity also enhanced from 1.6 to 4.7 mg/g in this MB concentration range. However, at the initial concentration of 80 mg/L, the treatment efficiency tended to decline sharply. This result was explained because the active sites of the adsorbent decreased compared to the increasing MB concentration. In contrast, the adsorption capacity continued to increase as MB concentration increased from 60 to 80 mg/L. According to Assimeddine et al. (2022), increasing the initial MB concentration improves the interaction between the MB molecules and the biochar particles, resulting in an increase in adsorption capacity. A similar trend was also reported in previous studies (Dawood et al., 2016; Phihusut and Chantharat, 2017; Subratti et al., 2021) on dye adsorption of biochar. In general, raising the concentration of MB enhanced adsorption capacity but decreased MB removal efficiency. Therefore, in this case, the appropriate initial MB concentration for the study was 50 mg/L. At this concentration, the removal efficiency reached 94.3±1.5%.

3.2.5 Adsorption isotherms

In essence, adsorption isotherms describe the relationship between MB concentration and adsorption capacity for a given biochar dose and temperature. Various isotherm models were applied to fit the experimental data and assess their usefulness for adsorption (Ayawei et al., 2017). In this study, the experimental data points were compared to theoretical Langmuir and Freundlich isotherms due to the simplicity of their model parameters. It can be seen in Figure 5 that Langmuir model symbolled the adsorption process on biochar better than Freundlich

model did because its values were close to the experimental value. In contrast, the values in the Freundlich model deviate further from the experimental value rendering it unsuitable. In addition, the parameters and correlation coefficients of these two isotherm models provided in Table 2 confirmed that the studied adsorption process fitted to the Langmuir model due to its higher correlation coefficient (R^2). Therefore, the monolayer adsorption occurred and the adsorption sites are identical and energetically equivalent.

Table 2. The parameters of the Langmuir and Freundlich isotherm models for MB adsorbed onto BSS at 30±2°C

Isotherm models	Parameters value	Correlation coefficient (R^2)
Langmuir	Q_m = 6.6 (mg/g) K_L = 0.414 (L/g)	0.897
Freundlich	n = 2.4 K_F = 0.332 × [(mg/g)/(mg/L)$^{1/n}$]	0.725

Table 3 shows the comparison of the MB absorption capabilities of BSS to those of other adsorbents. It was well known that there are many factors influencing the adsorbent capacity of biochar, such as its surface property and particle size, adsorbate and solution properties, and temperature. Therefore, the comparison between the adsorption capacity of BSS biochar and other types of adsorbents was difficult because of their different research conditions. However, the adsorption capability of biochar generated in this study outperformed that of biochar derived from pine wood, coir pith carbon, and eucalyptus (Kavitha and Namasivayam, 2007; Lonappan et al., 2016; Sun et al., 2013).

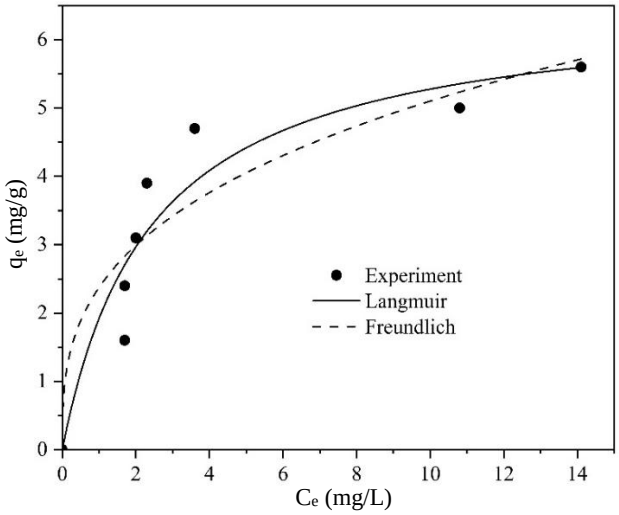

Figure 5. The adsorption isotherm models of MB dye onto BSS at 30±2°C

Table 3. The adsorption capabilities of various adsorbents for the elimination of MB dye

Adsorbents	Pyrolysis temperature (°C)	Heating time (h)	Q_{max} (mg/g)	References
Sesbania sesban	300	1	6.6	This research
Cedrela odorata (capsule-like interior)	400	1	158.5	Subratti et al. (2021)
Pine wood	525	-	3.9	Lonappan et al. (2016)
Eucalyptus	400	1	2.1	Sun et al. (2013)
Coir pith carbon	700	1	5.8	Kavitha and Namasivayam (2007)

3.2.6 Adsorption kinetic

The two kinetic models namely, pseudo-first-order and pseudo-second-order, have been analyzed to find out the kinetics and mechanism of the MB adsorption process. The results of the kinetic models are illustrated in Figure 6 and Table 4. According to the results, the two models matched the experimental data well, with a high correlation coefficient. However, chi-square values (χ^2) were analyzed to determine the best-fit kinetic models. The χ^2 values were near zero when the data derived using models were similar to that in (Ho and Wang, 2008). The constants, correlation coefficients, and χ^2 values of the kinetic models were shown in Table 4. The chi-square values of the pseudo-second-order (χ^2=0.001) were significantly lower than the pseudo-first-order (χ^2=2.106). Thus, the pseudo-second-order model was more correct in describing the adsorption process of BSS, whereas the pseudo-first-order model can only be suitable to describe the kinetics in the early stages of the adsorption process.

Table 4. The kinetic parameters for MB adsorption by BSS (non-linearized method)

Kinetic models	Parameters value	R^2	χ^2
Pseudo-first-order	$q_{e,exp}$ = 3.5 (mg/g) $q_{e,cal}$ = 3.5 (mg/g) k_1 = 0.29 (1/min)	0.999	2.106
Pseudo-second-order	$q_{e,exp}$ = 3.5 (mg/g) $q_{e,cal}$ = 3.6 (mg/g) k_2 = 0.39 (g/mg/min)	0.999	0.001

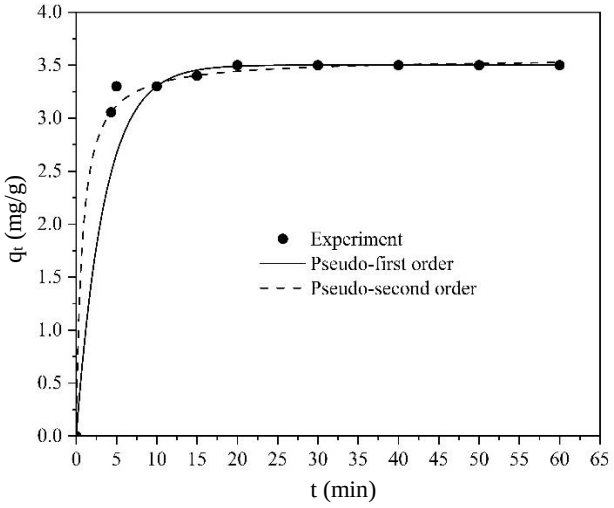

Figure 6. The adsorption kinetic models of MB dye onto BSS

4. CONCLUSION

Slow temperature pyrolysis resulted in BSS with a larger specific surface area and a more complex pore structure, indicating a strong adsorption potential. The adsorption factors, namely, initial pH, contact time, biochar dosage, and MB concentration, all had a substantial impact on MB adsorption. The equilibrium data fit well to the Langmuir isotherm model with the maximum adsorption capacity of 6.6 mg/g. The reaction achieved equilibrium in 30 minutes, and the adsorption kinetics followed the pseudo-second-order model. In general, the current investigation has demonstrated that the BSS looks to be a promising adsorbent candidate for the decolorization of dye-containing effluents. Furthermore, the BSS can be regenerated using the proper processes. If it is not economically feasible to regenerate the BSS, it must be treated according to hazardous waste procedures. Therefore, the regeneration of BSS also needs to be further studied to find an economically appropriate method and efficient reuse of materials.

ACKNOWLEDGEMENTS

The authors would like to thank the Center Laboratory of Research Institute for Sustainable Development, Ho Chi Minh University of Natural Resources and Environment for providing research facilities.

REFERENCES

Abdul RAR, Mohsin HM, Chin KBL, Johari K, Saman N. Promising low-cost adsorbent from desiccated coconut waste for removal of Congo red dye from aqueous solution. Water, Air, and Soil Pollution 2021;232(9):1-11.

Ahmad A, Khan N, Giri BS, Chowdhary P, Chaturvedi P. Removal of methylene blue dye using rice husk, cow dung and sludge biochar: Characterization, application, and kinetic studies. Bioresource Technology 2020;306:Article No. 123202.

Alorabi AQ, Hassan MS, Alam MM, Zabin SA, Alsenani NI, Baghdadi NE. Natural clay as a low-cost adsorbent for crystal violet dye removal and antimicrobial activity. Nanomaterials 2021;11(11):Article No. 2789.

Assimeddine M, Abdennouri M, Barka N, Elmoubarki R, Sadiq Mh. Natural phosphates characterization and evaluation of their removal efficiency of methylene blue and methyl orange from aqueous media. Environment and Natural Resources Journal 2022;20(1):29-41.

Ayawei N, Ebelegi AN, Wankasi D. Modelling and interpretation of adsorption isotherms. Journal of Chemistry 2017;2017: Article No. 3039817.

Bhattacharya S, Bar N, Rajbansi B, Das SK. Adsorptive elimination of Cu (II) from aqueous solution by chitosan-nanoSiO_2 nanocomposite: Adsorption study, MLR, and GA modeling. Water, Air, and Soil Pollution 2021;232(4):1-23.

Dan TH, Chiem NH, Brix H. Treatment of high-strength wastewater in tropical constructed wetlands planted with *Sesbania sesban*: Horizontal subsurface flow versus vertical downflow. Ecological Engineering 2011;37(5):711-20.

Dawood S, Sen TK, Phan C. Adsorption removal of Methylene blue (MB) dye from aqueous solution by bio-char prepared from *Eucalyptus sheathiana* bark: Kinetic, equilibrium, mechanism, thermodynamic and process design. Desalination and Water Treatment 2016;57(59):28964-80.

Du PD, Danh HT. Single and binary adsorption systems of Rhodamine B and methylene blue onto alkali-activated Vietnamese diatomite. Adsorption Science and Technology 2021;2021:Article No. 1014354.

Farghaly MM, Youssef IM, Radwan MA, Hamdon HA. Effect of feeding *Sesbania sesban* and reed grass on growth performance, blood parameters, and meat quality of growing lambs. Tropical Animal Health and Production 2022;54(1):1-13.

Hameed B, Ahmad A, Latiff K. Adsorption of basic dye (methylene blue) onto activated carbon prepared from rattan sawdust. Dyes and Pigments 2007;75(1):143-9.

Ho YS, Wang CC. Sorption equilibrium of mercury onto ground-up tree fern. Journal of Hazardous Materials 2008;156(1-3):398-404.

Huang W, Chen J, Zhang J. Adsorption characteristics of methylene blue by biochar prepared using sheep, rabbit, and pig manure. Environmental Science and Pollution Research 2018;25(29):29256-66.

Hussain Z, Chang N, Sun J, Xiang S, Ayaz T, Zhang H, et al. Modification of coal fly ash and its use as low-cost adsorbent for the removal of directive, acid and reactive dyes. Journal of Hazardous Materials 2022;422:Article No. 126778.

Inyang M, Gao B, Zimmerman A, Zhang M, Chen H. Synthesis, characterization, and dye sorption ability of carbon nanotube-biochar nanocomposites. Chemical Engineering Journal 2014;236:39-46.

Joseph J, Radhakrishnan RC, Johnson JK, Joy SP, Thomas J. Ion-exchange mediated removal of cationic dye-stuffs from water using ammonium phosphomolybdate. Materials Chemistry and Physics 2020;242:Article No. 122488.

Kavitha D, Namasivayam C. Experimental and kinetic studies on methylene blue adsorption by coir pith carbon. Bioresource Technology 2007;98(1):14-21.

Khayat Z, Zali-Boeini H. Phase selective amphiphilic super-gelators for oil spill solidification and dye removal. Soft Materials 2019;17(2):150-8.

Kwesiga F, Franzel S, Place F, Phiri D, Simwanza C. *Sesbania sesban* improved fallows in eastern Zambia: Their inception, development and farmer enthusiasm. Agroforestry Systems 1999;47(1):49-66.

Lee T, Nam IH, Jung S, Park YK, Kwon EE. Synthesis of nickel/biochar composite from pyrolysis of *Microcystis aeruginosa* and its practical use for syngas production. Bioresource Technology 2020;300:Article No. 122712.

Li Y, Du Q, Liu T, Peng X, Wang J, Sun J, et al. Comparative study of methylene blue dye adsorption onto activated carbon, graphene oxide, and carbon nanotubes. Chemical Engineering Research and Design 2013;91(2):361-8.

Liu H, Zhang J, Lu M, Liang L, Zhang H, Wei J. Biosynthesis based membrane filtration coupled with iron nanoparticles reduction process in removal of dyes. Chemical Engineering Journal 2020;387:Article No. 124202.

Liu Y, Zhao X, Li J, Ma D, Han R. Characterization of bio-char from pyrolysis of wheat straw and its evaluation on methylene blue adsorption. Desalination and Water Treatment 2012; 46(1-3):115-23.

Lonappan L, Rouissi T, Das RK, Brar SK, Ramirez AA, Verma M, et al. Adsorption of methylene blue on biochar microparticles derived from different waste materials. Waste Management 2016;49:537-44.

Meyer S, Glaser B, Quicker P. Technical, economical, and climate-related aspects of biochar production technologies: A literature review. Environmental Science and Technology 2011;45(22):9473-83.

Misran E, Bani O, Situmeang EM, Purba AS. Banana stem based activated carbon as a low-cost adsorbent for methylene blue removal: Isotherm, kinetics, and reusability. Alexandria Engineering Journal 2022;61(3):1946-55.

Nguyen XC, Nguyen TTH, Nguyen THC, Van Le Q, Vo TYB, Tran TCP, et al. Sustainable carbonaceous biochar adsorbents derived from agro-wastes and invasive plants for cation dye adsorption from water. Chemosphere 2021;282:Article No. 131009.

Nodehi R, Shayesteh H, Rahbar-Kelishami A. Fe_3O_4@ NiO core-shell magnetic nanoparticle for highly efficient removal of Alizarin red S anionic dye. International Journal of Environmental Science and Technology 2022;19(4):2899-912.

Nouri H, Azin E, Kamyabi A, Moghimi H. Biosorption performance and cell surface properties of a fungal-based sorbent in azo dye removal coupled with textile wastewater. International Journal of Environmental Science and Technology 2021;18(9):2545-58.

Oussalah A, Boukerroui A. Alginate-bentonite beads for efficient adsorption of methylene blue dye. Euro-Mediterranean Journal for Environmental Integration 2020;5(2):1-10.

Phihusut D, Chantharat M. Removal of methylene blue using agricultural waste: A case study of rice husk and rice husk ash from chaipattana rice mill demonstration center. Environment and Natural Resources Journal 2017;15(2):30-8.

Rahman-Setayesh MR, Rahbar Kelishami A, Shayesteh H. Equilibrium, kinetic, and thermodynamic applications for methylene blue removal using *Buxus sempervirens* leaf powder as a powerful low-cost adsorbent. Journal of Particle Science and Technology 2019;5(4):161-70.

Rashidi HR, Sulaiman NMN, Hashim NA, Hassan CRC, Ramli MR. Synthetic reactive dye wastewater treatment by using nano-membrane filtration. Desalination and Water Treatment 2015;55(1):86-95.

Rodríguez-Narváez OM, Picos AR, Bravo-Yumi N, Pacheco-Alvarez M, Martínez-Huitle CA, Peralta-Hernández JM. Electrochemical oxidation technology to treat textile wastewaters. Current Opinion in Electrochemistry 2021; 29:Article No. 100806.

Saleh AK, El-Gendi H, Ray JB, Taha TH. A low-cost effective media from starch kitchen waste for bacterial cellulose production and its application as simultaneous absorbance for methylene blue dye removal. Biomass Conversion and Biorefinery 2021;preprint:1-13.

Sarbisheh F, Norouzbeigi R, Hemmati F, Shayesteh H. Application of response surface methodology for modeling and optimization of malachite green adsorption by modified sphagnum peat moss as a low cost biosorbent. Desalination and Water Treatment 2017;59:230-42.

Shayesteh H, Rahbar-Kelishami A, Norouzbeigi R. Evaluation of natural and cationic surfactant modified pumice for congo red removal in batch mode: Kinetic, equilibrium, and thermodynamic studies. Journal of Molecular Liquids 2016;221:1-11.

Subratti A, Vidal JL, Lalgee LJ, Kerton FM, Jalsa NK. Preparation and characterization of biochar derived from the fruit seed of *Cedrela odorata* L. and evaluation of its adsorption capacity with methylene blue. Sustainable Chemistry and Pharmacy 2021;21:Article No. 100421.

Sun L, Wan S, Luo W. Biochars prepared from anaerobic digestion residue, palm bark, and eucalyptus for adsorption of cationic methylene blue dye: Characterization, equilibrium, and kinetic studies. Bioresource Technology 2013;140:406-13.

Sutar S, Patil P, Jadhav J. Recent advances in biochar technology for textile dyes wastewater remediation: A review. Environmental Research 2022;209:Article No. 112841.

Tehubijuluw H, Subagyo R, Yulita MF, Nugraha RE, Kusumawati Y, Bahruji H, et al. Utilization of red mud waste into mesoporous ZSM-5 for methylene blue adsorption-desorption studies. Environmental Science and Pollution Research 2021;28(28):37354-70.

Tran TH, Le AH, Pham TH, Nguyen DT, Chang SW, Chung WJ, et al. Adsorption isotherms and kinetic modeling of methylene

blue dye onto a carbonaceous hydrochar adsorbent derived from coffee husk waste. Science of the Total Environment 2020;725:Article No. 138325.

Zhang W, Zhou C, Zhou W, Lei A, Zhang Q, Wan Q, et al. Fast and considerable adsorption of methylene blue dye onto graphene oxide. Bulletin of Environmental Contamination and Toxicology 2011;87(1):86-90.